

Supplementary Information

Donor Position Driven Excited State Modulation in Benzoylthiophene-Carbazole Emitters: Divergent TTA/RTP Pathway for High Efficiency Blue-Cyan OLEDs

Ajeet Kumar Sharma,^{a,±} Prasannamani Govindharaj,^{b,±} K. R. Justin Thomas,^{a,*} Przemyslaw
Data,^{b,*}

^a Organic Materials Laboratory, Department of Chemistry, Indian Institute of Technology
Roorkee, Roorkee – 247667, India.

^b Department of Molecular Physics, Faculty of Chemistry, Łódź University of Technology, 90-
543 Łódź, Poland

* Corresponding authors: krjt@cy.iitr.ac.in; przemyslaw.data@p.lodz.pl

Supplementary Information

Experimental Section	S3
General methods	S3
Theoretical Computations	S3
OLED Device Fabrication	S3
Synthesis	S4
Figure S1	(a) Absorption, (b) emission spectra of the bromo derivatives, 2a , 2b and 2c recorded in DCM. S6
Table S1	Absorption, emission spectral data of the 2a , 2b and 2c recorded in 1×10^{-4} M and 1×10^{-5} M DCM solution, respectively. S7
Figure S2	(a) Absorption, (b) emission spectra of 4a recorded in different solvents and (c) visual image of the excited (365 nm) 4a in different solvents. S7
Figure S3	(a) Absorption spectra of 4b recorded in different solvents, (b) absorption spectra of the dye 4b recorded in toluene/DCM solvents and (c) visual image of the excited (365 nm) 4b in different solvents. S8

Figure S4	(a) Absorption, (b) emission spectra of 4c recorded in different solvents and (c) visual image of the excited (365 nm) 4c in different solvents.	S9
Table S2	Solvatochromic data of 4a in various solvents.	S9
Table S3	Solvatochromic data of 4b in various solvents.	S10
Table S4	Solvatochromic data of 4c in various solvents.	S10
Figure S5	visual image of the excited (365 nm) 4c in toluene/DCM binary solvent.	S10
Figure S6	Photoexcited at 365nm image of the dyes 4a , 4b and 4c drop-cast thin films.	S11
Figure S7	Changes in the emission observed on changing the water ratio in THF for the dyes (a) 4a , (b) 4b , and (c) 4c .	S11
Figure S8	Visual images of the photoexcited (365 nm) dyes (a) 4a , (b) 4b , (c) 4c in different water ratios in THF.	S12
Figure S9	SEM images of 4a in powder and aggregated forms obtained from different water ratio.	S12
Figure S10	Cyclic voltammograms of 1 mM of emitter (4a-4c) in 0.1 M Bu ₄ NBF ₄ in DCM electrolyte at a scan rate of 50 mV/s.	S13
Table S5	Electrochemical parameters extracted from cyclic voltammograms.	S13
Figure S11	Steady-state PL emission of 4a-4c in ambient condition: 1 wt% of emitter in Zeonex (a); 10 wt% of emitters in CBP; PLQY was measured at ambient condition. Spectra were recorded at 300K using $\lambda_{ex} = 355$ nm.	S14
Figure S12	Steady-state photoluminescence (PL) spectra in Zeonex® in the presence of air (Under air) and in a vacuum (degassed). Recorded at 300 K using $\lambda_{ex}=355$ nm.	S14
Figure S13	Temperature dependent time resolved PH spectra of the 1wt% of emitters (4a-4c) in Zeonex. (a-c) and $\lambda_{ex}=355$ nm.	S15
Figure S14	Differential scanning calorimetry (DSC) traces of 4a , 4b and 4c .	S15
Figure S15	Energy level diagram of 4a .	S15
Figure S16	Emission NTO analysis of 4a .	S16
Figure S17	Energy level diagram of 4b .	S16
Figure S18	Emission NTO analysis of 4b .	S17
Table S6	Crystal data and structure refinement data for 4a .	S18
Table S7	Crystal data and structure refinement data for 4b .	S19
Table S8	Crystal data and structure refinement data for 4c .	S20
Figure S19	¹ H NMR spectrum of 2a recorded in CDCl ₃ .	S21
Figure S20	¹ H NMR spectrum of 2b recorded in CDCl ₃ .	S22
Figure S21	¹³ C NMR spectrum of 2b recorded in CDCl ₃ .	S23
Figure S22	¹ H NMR spectrum of 2c recorded in CDCl ₃ .	S24
Figure S23	¹³ C NMR spectrum of 2c recorded in CDCl ₃ .	S25
Figure S24	¹ H NMR spectrum of 4a recorded in CDCl ₃ .	S26
Figure S25	¹³ C NMR spectrum of 4a recorded in CDCl ₃ .	S27
Figure S26	¹ H NMR spectrum of 4b recorded in CDCl ₃ .	S28
Figure S27	¹³ C NMR spectrum of 4b recorded in CDCl ₃ .	S29
Figure S28	¹ H NMR spectrum of 4c recorded in CDCl ₃ .	S30
Figure S29	¹³ C NMR spectrum of 4c recorded in CDCl ₃ .	S31

Experimental section

General Methods

All chemicals were obtained from commercial suppliers and used without further purification unless otherwise noted. Solvents were dried by standard distillation methods prior to use. Organic products were purified by column chromatography on silica gel (100–200 mesh). ^1H and ^{13}C NMR spectra were recorded on a JEOL 400 MHz spectrometer at 298 K in CDCl_3 , with tetramethylsilane (TMS) as an internal standard. High-resolution mass spectra (HRMS) were acquired using a high-resolution mass spectrometer. UV–Vis absorption spectra were measured on a Cary 100 UV–Vis spectrophotometer, while fluorescence emission spectra were recorded using a Shimadzu spectrofluorometer. Fluorescence quantum yields were determined with a calibrated integrating sphere attached to the same instrument. Thermal properties were evaluated using a PerkinElmer Pyris Diamond thermogravimetric analyzer (TGA) and a Shimadzu DSC-60 Plus differential scanning calorimeter (DSC) under a nitrogen atmosphere at a heating rate of $10\text{ }^\circ\text{C}\cdot\text{min}^{-1}$. FTIR spectra were collected on a PerkinElmer Spectrum 2 spectrophotometer in the range of $400\text{--}4000\text{ cm}^{-1}$. Morphological analyses were performed using a Carl Zeiss Ultra Plus field-emission scanning electron microscope (FE-SEM)

Theoretical Computations

All computational calculations for dyes **4a**, **4b**, and **4c** were performed using the ORCA 5.0.4 package. Ground-state geometries of the compounds were optimized at the B3LYP/def2-svp level of theory under vacuum. Frequency calculations were performed and found no negative frequencies. Time-dependent DFT (TD-DFT) calculations were carried out at the same functional with def2-tzvp basis set to determine vertical excitation energies and oscillator strengths. The charge transfer indices and related parameters were estimated using Multiwfn software.

OLED Device Fabrication

OLEDs were constructed on patterned ITO/glass substrates (100 nm, $20\ \Omega/\text{sq}$) following established procedures.¹ The device stack comprised HAT CN (hole injection), NPB (hole transport), CBP:10 wt% emitter (emissive layer), TmPyPB (electron transport), and LiF/Al cathodes. Organic layers and Al were deposited at $1\ \text{\AA}\ \text{s}^{-1}$, while LiF was deposited at $0.1\ \text{\AA}\ \text{s}^{-1}$, using a Kurt J. Lesker Spectros thermal evaporator under 10^{-7} mbar without breaking vacuum. All

materials (Sigma Aldrich, Lumtec) were purified by gradient sublimation. Pixel areas of 4, 8 and 16 mm² were fabricated. Device performance was measured with a Labsphere integrating sphere coupled to a source meter and Ocean Optics USB4000 spectrometer inside a glovebox.

Synthesis

(5-bromothiophen-2-yl)(phenyl) methanone (2a)¹

A mixture of benzoyl chloride (2.81 g, 20.0 mmol) and 2-bromothiophene (3.42 g, 21.0 mmol) in DCM (50 mL) was cooled in an ice bath, and AlCl₃ (5.34 g, 40.0 mmol) was added portionwise over 10 min under vigorous stirring. The reaction mixture was then stirred at room temperature for 2-4 h and quenched with 1 M HCl (aq., 100 mL). The resulting mixture was filtered under reduced pressure, and the layers were separated. The aqueous phase was extracted with DCM (3 × 50 mL). The combined organic extracts were washed with water (3 × 100 mL), dried over anhydrous Na₂SO₄, filtered, and concentrated in vacuo. The crude product was purified by silica gel column chromatography using 10-12% DCM/hexane as the eluent to afford the product as a light yellow solid (9.6 g, 87%). ¹H NMR (500 MHz, CDCl₃, δ): 7.82 (dt, J = 8.4, 1.7 Hz, 2H), 7.60 (m, 1H), 7.50 (m, 2H), 7.38 (d, J = 4.0 Hz, 1H), 7.13 (d, J = 4.0 Hz, 1H).

(4-bromothiophen-2-yl)(phenyl)methanone (2b) / (3-bromothiophen-2-yl)(phenyl) methanone (2c)

A mixture of benzoyl chloride (5.62 g, 40 mmol) and 3-bromothiophene (7.68 g, 42 mmol) in DCM (80 mL) was cooled in an ice bath, and AlCl₃ (10.68 g, 80 mmol) was added portionwise over 10 min under vigorous stirring. The reaction mixture was then stirred at room temperature for 2-4 h and quenched with 1 M HCl (aq., 100 mL). The mixture was filtered under reduced pressure, and the layers were separated. The aqueous layer was extracted with DCM (3×50 mL). The combined organic extracts were washed with water (3×100 mL), dried over anhydrous Na₂SO₄, filtered, and concentrated in vacuo. The crude product was purified by silica gel column chromatography using 1-3% ethyl acetate/hexane as the eluent to afford the desired product.

(4-bromothiophen-2-yl)(phenyl)methanone (**2b**). White solid. Yield 1.9g (18%). ¹H NMR (500 MHz, CDCl₃, δ): 7.85 (d, J = 8.0 Hz, 2H), 7.62 (m, 2H), 7.53 (dd, J = 12.9, 4.4 Hz, 3H). ¹³C NMR (500 MHz, CDCl₃, δ): 187.09 (s), 144.08 (s), 137.30 (s), 136.57 (s), 132.85 (s), 131.47 (s),

129.25 (s), 128.71 (s), 110.87 (s). HRMS (ESI) m/z : $[M + H]^+$ calcd for $C_{11}H_7OS$, 266.9479; found, 266.9475.

(3-bromothiophen-2-yl)(phenyl)methanone (**2c**). Yellow liquid. Yield 8.58g (80%). 1H NMR (500 MHz, $CDCl_3$, δ): 7.84 (d, $J = 7.6$ Hz, 2H), 7.60 (t, $J = 7.4$ Hz, 1H), 7.56 (d, $J = 5.2$ Hz, 1H), 7.48 (t, $J = 7.7$ Hz, 2H), 7.14 (d, $J = 5.2$ Hz, 1H). ^{13}C NMR (500 MHz, $CDCl_3$, δ): 188.19 (s), 137.83 (s), 135.82 (s), 133.10 (s), 132.86 (s), 131.22 (s), 129.82 (s), 128.47 (s), 115.33 (s). HRMS (ESI) m/z : $[M + H]^+$ calcd for $C_{11}H_7OS$, 266.9479; found, 266.9482.

(5-(4-(9H-carbazol-9-yl)phenyl)thiophen-2-yl)(phenyl)methanone (4a)

A mixture of **2a** (0.50 g, 1.87 mmol), (4-(9H-carbazol-9-yl)phenyl)boronic acid (0.59 g, 2.05 mmol), $Pd(PPh_3)_4$ (3 mol%), and K_2CO_3 (0.64 g, 4.68 mmol) was dissolved in a THF/water mixture (3:1 v/v) under an inert atmosphere. The reaction mixture was refluxed at 80 °C for 8 h. After completion (monitored by TLC), the mixture was cooled to room temperature and extracted with DCM. The combined organic layers were washed with brine, dried over anhydrous Na_2SO_4 , filtered, and concentrated under reduced pressure. The crude product was purified by silica gel column chromatography using 25–30% DCM/hexane as the eluent to give a light yellow solid (0.70 g, 87%). 1H NMR (500 MHz, $CDCl_3$, δ): 8.16 (d, $J = 7.7$ Hz, 2H), 7.92 (t, $J = 7.4$ Hz, 4H), 7.65 (dt, $J = 14.8, 5.9$ Hz, 4H), 7.54 (t, $J = 7.6$ Hz, 2H), 7.46 (dt, $J = 15.0, 8.1$ Hz, 5H), 7.32 (t, $J = 7.4$ Hz, 2H). ^{13}C NMR (500 MHz, $CDCl_3$, δ): 187.97 (s), 152.00 (s), 142.73 (s), 140.54 (s), 138.43 (s), 138.02 (s), 135.99 (s), 132.29 (s), 132.24 (s), 129.13 (s), 128.48 (s), 127.75 (s), 127.49 (s), 126.09 (s), 124.24 (s), 123.60 (s), 120.40 (s), 120.29 (s), 109.74 (s). HRMS (ESI) m/z : $[M + H]^+$ calcd for $C_{29}H_{19}NOS$, 430.1265; found, 430.1257.

(4-(4-(9H-carbazol-9-yl)phenyl)thiophen-2-yl)(phenyl)methanone (4b)

A mixture of **2b** (0.3 g, 1.12 mmol), (4-(9H-carbazol-9-yl)phenyl)boronic acid (**3**) (0.38 g, 1.34 mmol) and tetrakis(triphenylphosphine)palladium(0) (3 mol%) and potassium carbonate (0.37 g, 2.69 mmol) were taken in a mixture of THF:water (3:1 volume ratio) under inert atmosphere. Same procedure was followed as per given in synthesis of **4a**. The obtained residue was purified by column chromatography (20-25% DCM/Hexane). White solid. Yield 0.41 g (85%). 1H NMR (500 MHz, $CDCl_3$, δ): 8.16 (dt, $J = 7.8, 1.0$ Hz, 2H), 7.99 (d, $J = 1.5$ Hz, 1H), 7.95 (m, 3H), 7.81 (m), 7.64 (m), 7.56 (m), 7.44 (m), 7.31 (ddd, $J = 8.0, 6.5, 1.7$ Hz). ^{13}C NMR (500 MHz, $CDCl_3$, δ): 188.33 (s), 144.51 (s), 142.40 (s), 140.77 (s), 138.01 (s), 137.32 (s), 133.94 (s), 133.39 (s),

132.64 (s), 129.34 (s), 129.26 (s), 128.70 (s), 127.90 (s), 127.62 (s), 126.11 (s), 123.54 (s), 120.49 (s), 120.20 (s), 109.80 (s). HRMS (ESI) m/z : $[M + H]^+$ calcd for $C_{29}H_{19}NOS$, 430.1265; found, 430.1254.

(3-(4-(9H-carbazol-9-yl)phenyl)thiophen-2-yl)(phenyl)methanone (4c)

A mixture of **2c** (0.3 g, 1.12 mmol), (4-(9H-carbazol-9-yl)phenyl)boronic acid (**3**) (0.38 g, 1.34 mmol) and tetrakis(triphenylphosphine)palladium(0) (3 mol%) and potassium carbonate (0.37 g, 2.69 mmol) were taken in a mixture of THF:water (3:1 volume ratio) under inert atmosphere. Same procedure was followed as per given in synthesis of **4a**. The obtained residue was purified by column chromatography (20-25% DCM/Hexane). Light yellow solid. Yield 0.39 g (81%). 1H NMR (500 MHz, $CDCl_3$, δ): 8.13 (ddd, $J = 7.8, 1.3, 0.8$ Hz), 7.74 (t, $J = 4.9$ Hz), 7.67 (m), 7.41 (m), 7.34 (m), 7.29 (m), 7.27 (m), 7.25 (dd, $J = 1.3, 0.9$ Hz), 7.22 (m). ^{13}C NMR (500 MHz, $CDCl_3$, δ): 190.32 (s), 145.89 (s), 140.76 (s), 138.05 (s), 137.79 (s), 137.20 (s), 134.87 (s), 132.53 (s), 131.26 (s), 130.87 (s), 130.47 (s), 129.93 (s), 128.03 (s), 126.73 (s), 125.94 (s), 123.45 (s), 120.40 (s), 120.11 (s), 109.78 (s). HRMS (ESI) m/z : $[M + H]^+$ calcd for $C_{29}H_{19}NOS$, 430.1265; found, 430.1263.

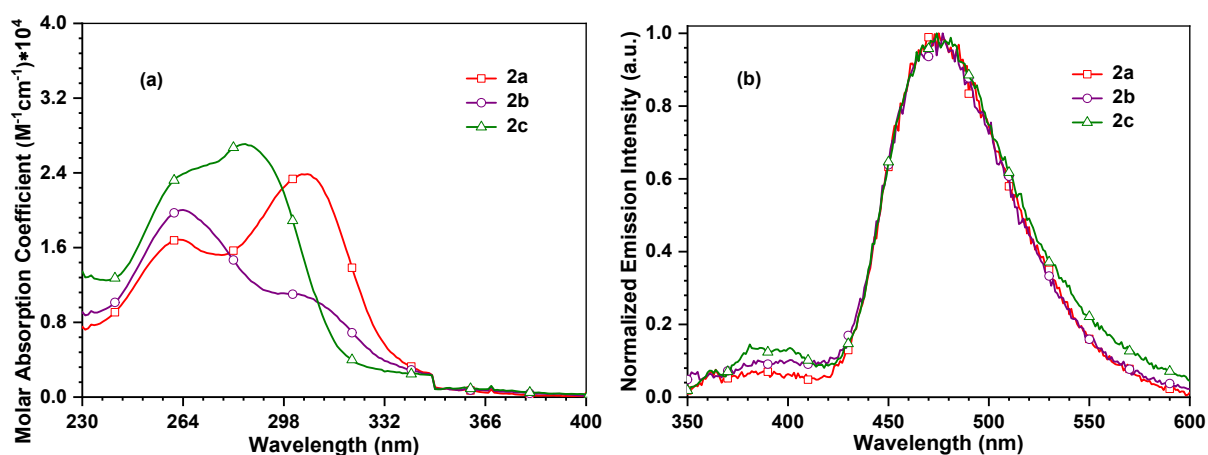
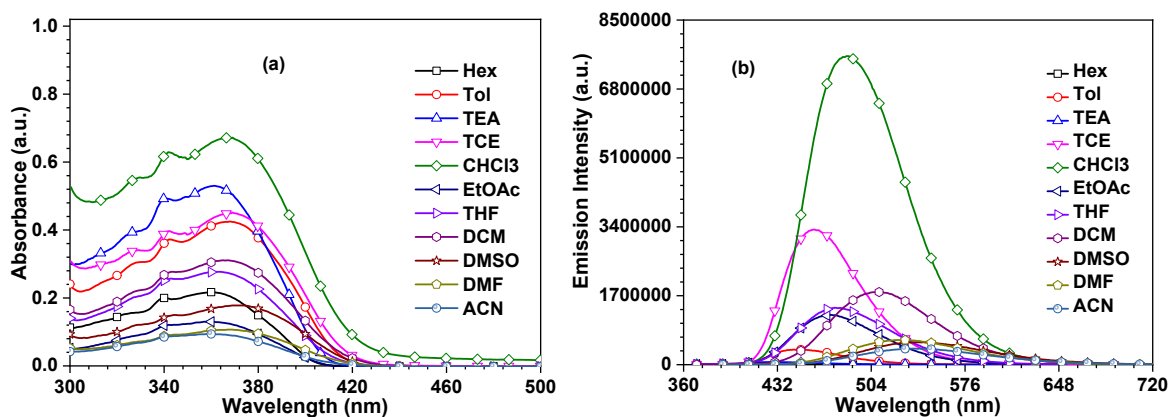


Figure S1. (a) Absorption, (b) emission spectra of the bromo derivatives, **2a**, **2b** and **2c** recorded in DCM.

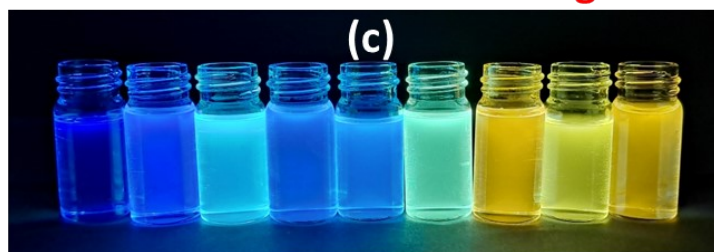
Table S1. (a) Absorption and emission spectral data of the **2a**, **2b** and **2c** recorded in 1×10^{-4} M and 1×10^{-5} M DCM solution, respectively.

Compounds	λ_{abs} (nm) ($\epsilon_{\text{max}} \times 10^4$ ($\text{M}^{-1} \text{cm}^{-1}$)) ^a	λ_{em} (nm) ^a
2a	262(1.67), 305(2.37)	475
2b	262(1.99), 303(1.09)	475
2c	262(2.36), 285(2.69)	474

^a Measured in DCM solution.

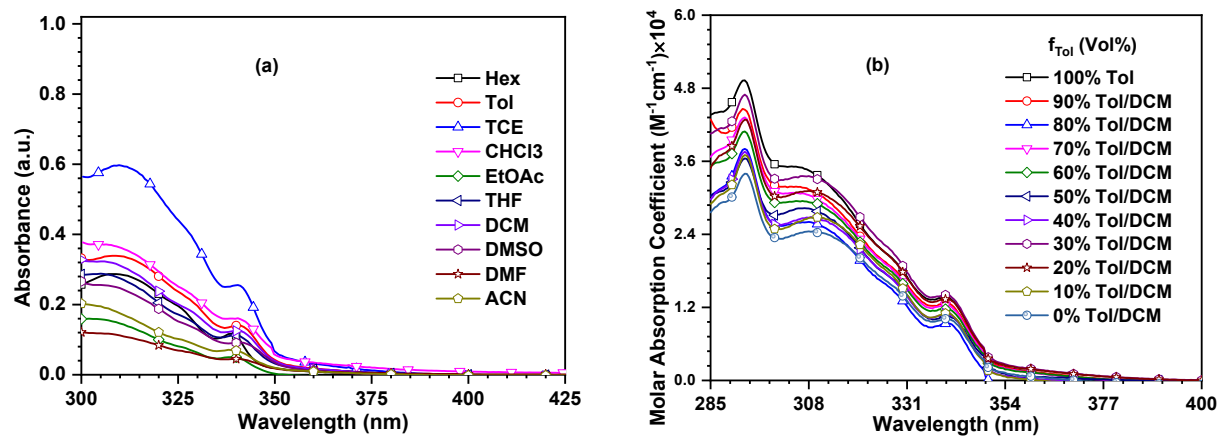


Low Polar \longrightarrow High Polar

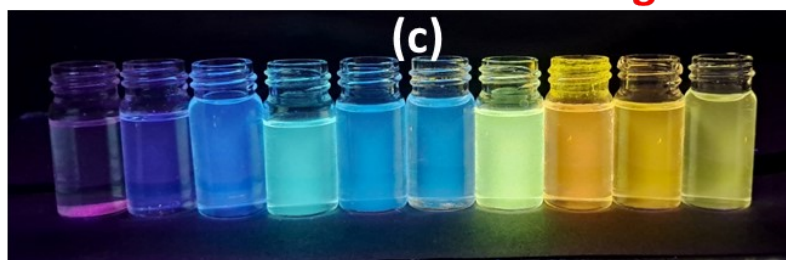


Tol, TCE, CHCl₃, EtOAc, THF, DCM, DMSO, DMF, ACN

Figure S2. (a) Absorption, (b) emission spectra of **4a** recorded in different solvents and (c) visual image of the excited (365 nm) **4a** in different solvents.

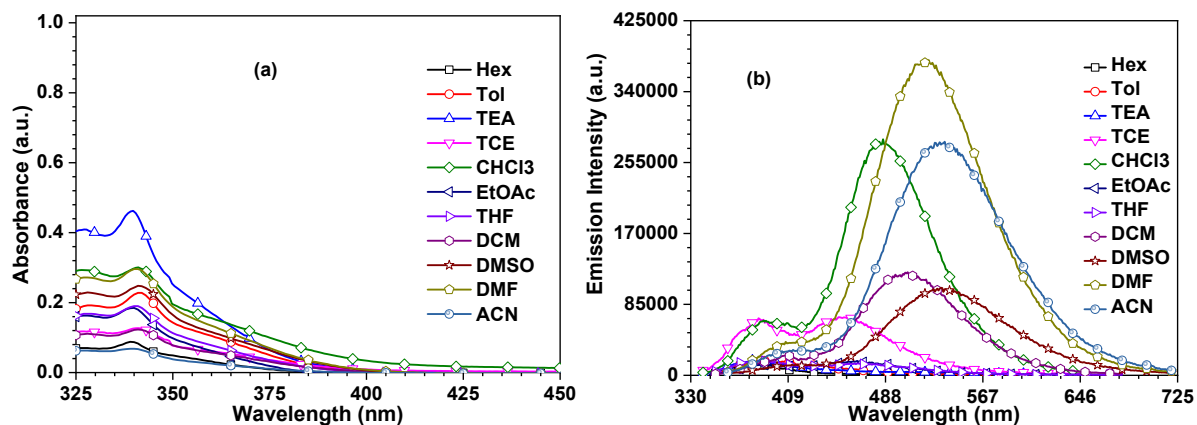


Low Polar \longrightarrow High Polar

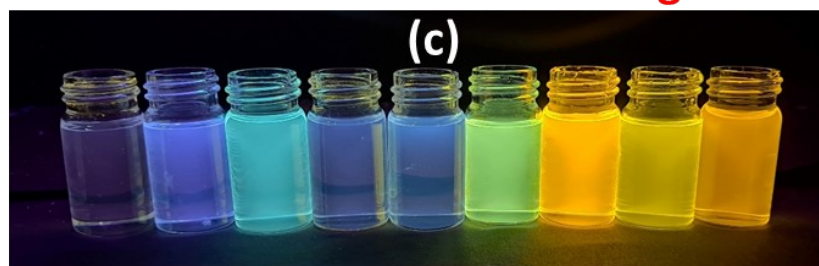


Hex, Tol, TCE, CHCl₃, EtOAc, THF, DCM, DMSO, DMF, ACN

Figure S3. (a) Absorption spectra of **4b** recorded in different solvents, (b) absorption spectra of the dye **4b** recorded in toluene/DCM solvents and (c) visual image of the excited (365 nm) **4b** in different solvents.



Low Polar \longrightarrow High Polar



Tol, TCE, CHCl₃, EtOAc, THF, DCM, DMSO, DMF, ACN

Figure S4. (a) Absorption, (b) emission spectra of **4c** recorded in different solvents and (c) visual image of the excited (365 nm) **4c** in different solvents.

Table S2. Solvatochromic data of **4a** in various solvents.

Solvent	E_N^T	Orientation Polarizability (Δf)	λ_{abs} (nm)	λ_{em} (nm)	Stokes Shift (nm)	$\Delta\nu$ (cm ⁻¹)	FWHM (nm)
Hex	0.009	0.0012	359	425	66	4325.7	61
TOL	0.099	0.014	367	448	81	4926.5	62
TEA	0.043	0.045	360	430	70	4521.9	63
TCE	0.160	0.085	369	460	91	5361.1	67
CHCl ₃	0.259	0.149	367	485	118	6629.4	84
EtOAc	0.228	0.199	360	472	112	6591.3	76
THF	0.207	0.210	363	478	115	6627.7	80
DCM	0.309	0.217	367	510	143	7714.5	91
DMSO	0.444	0.263	372	542	170	8431.5	107
DMF	0.386	0.276	368	529	161	8270.3	102
ACN	0.460	0.305	361	539	178	9147.9	111

Table S3. Solvatochromic data of **4b** in various solvents.

Solvent	E^N_T	Orientation Polarizability (Δf)	λ_{abs} (nm)	λ_{em} (nm)	Stokes Shift (nm)	$\Delta\nu$ (cm^{-1})	FWHM (nm)
Hex	0.009	0.0012	309	360	51	4738.1	48
TOL	0.099	0.014	309	367	58	5624.4	121
TCE	0.160	0.085	310	456	146	10328.2	75
CHCl ₃	0.259	0.149	306	488	182	11932.8	88
EtOAc	0.228	0.199	304	470	166	11618.1	78
THF	0.207	0.210	305	369	64	11645.2	156
DCM	0.309	0.217	305	510	205	13369.4	99
DMSO	0.444	0.263	305	547	242	14505.3	235
DMF	0.386	0.276	305	531	226	13954.4	111
ACN	0.460	0.305	305	542	237	14336.7	115

Table S4. Solvatochromic data of **4c** in various solvents.

Solvent	E^N_T	Orientation Polarizability (Δf)	λ_{abs} (nm)	λ_{em} (nm)	Stokes Shift (nm)	$\Delta\nu$ (cm^{-1})	FWHM (nm)
Hex	0.009	0.0012	339	383	44	3388.8	53
TOL	0.099	0.014	341	387	46	3485.7	55
TEA	0.043	0.045	339	389	50	3791.5	59
TCE	0.160	0.085	341	447	106	6954.1	135
CHCl ₃	0.259	0.149	341	481	140	8535.4	83
EtOAc	0.228	0.199	339	464	125	7946.8	132
THF	0.207	0.210	340	461	121	7719.7	121
DCM	0.309	0.217	341	505	164	9523.5	94
DMSO	0.444	0.263	341	535	194	10633	108
DMF	0.386	0.276	341	526	185	10314	104
ACN	0.460	0.305	340	532	192	10614	108

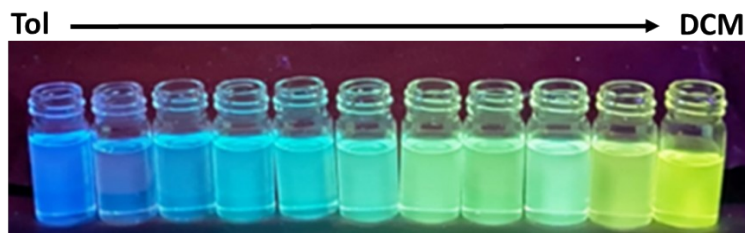


Figure S5. visual image of the excited (365 nm) **4c** in toluene/DCM binary solvent.



Figure S6. Photoexcited at 365nm image of the dyes **4a**, **4b** and **4c** drop-cast thin films.

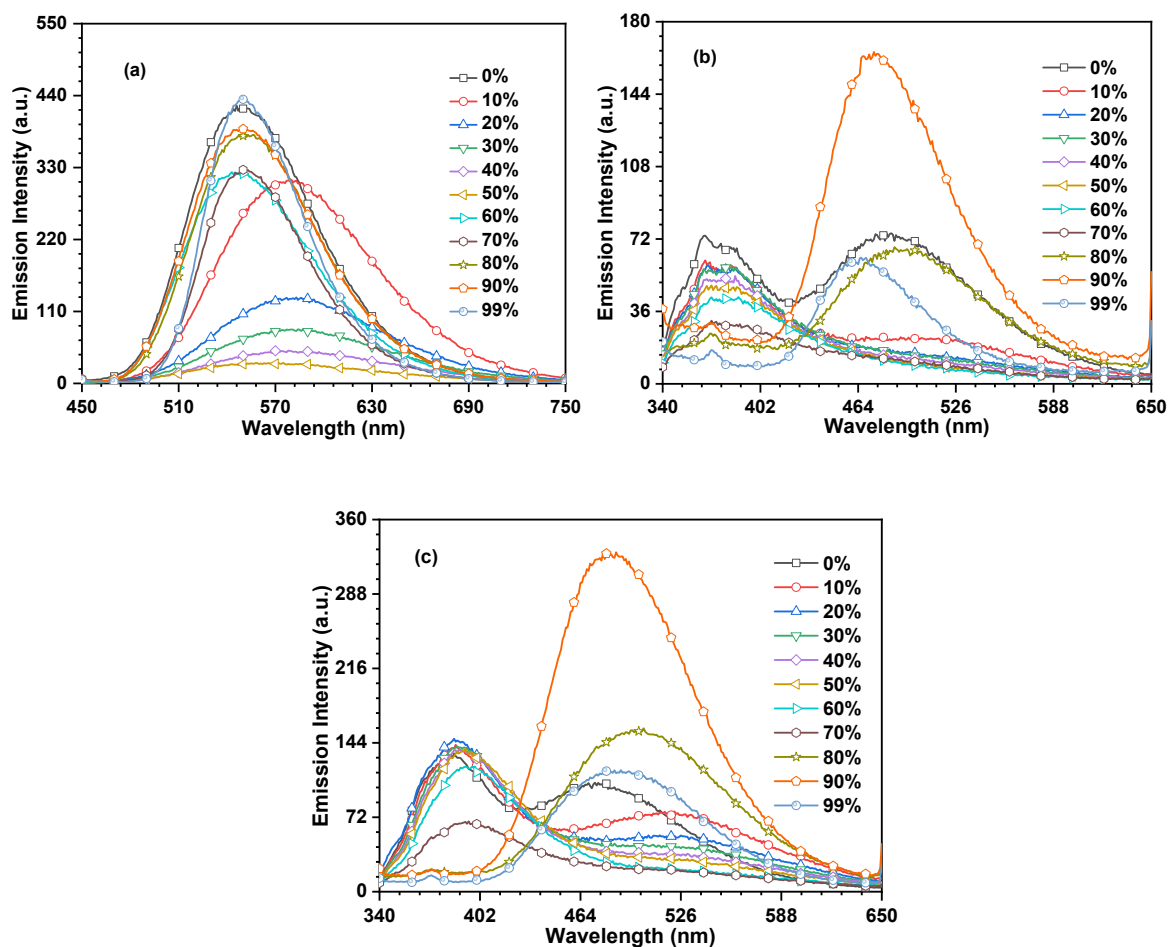


Figure S7. Changes in the emission observed on changing the water ratio in THF for the dyes (a) **4a**, (b) **4b**, and (c) **4c**.

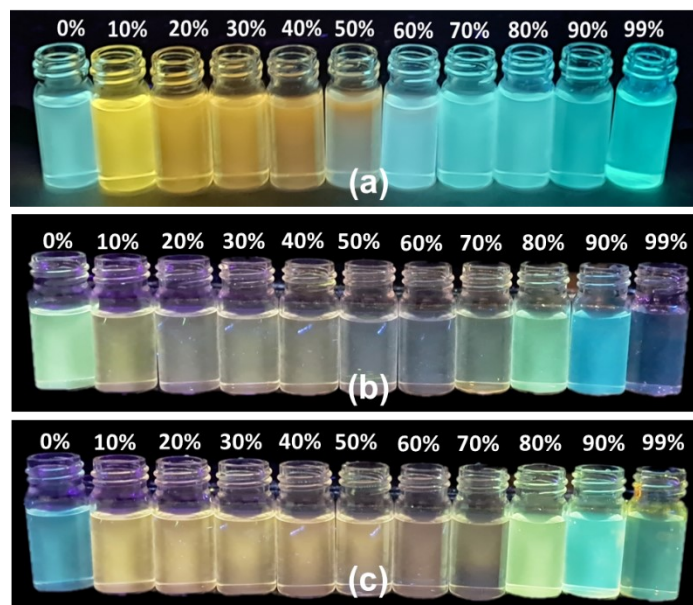


Figure S8. Visual images of the photoexcited (365 nm) dyes (a) **4a**, (b) **4b**, (c) **4c** in different water ratios in THF.

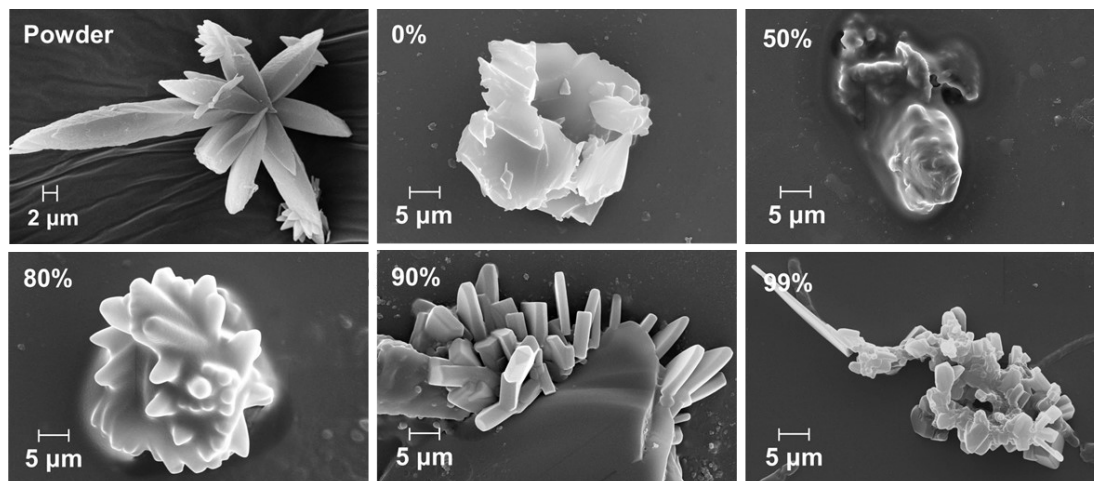


Figure S9. SEM images of **4a** in powder and aggregated forms obtained from different water ratio.

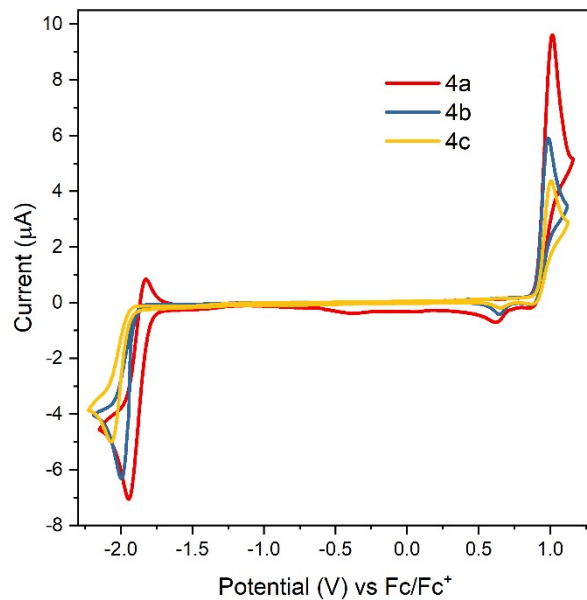


Figure S10. Cyclic voltammograms of 1 mM of emitter (**4a-4c**) in 0.1 M Bu_4NBF_4 in DCM electrolyte at a scan rate of 50 mV/s.

Table S5. Electrochemical parameters extracted from cyclic voltammograms.

Emitters	LUMO (eV)	HOMO (eV)	Band gap (eV)
4a	-3.31	-6.00	-2.69
4b	-3.20	-6.01	-2.81
4c	-3.18	-6.02	-2.84

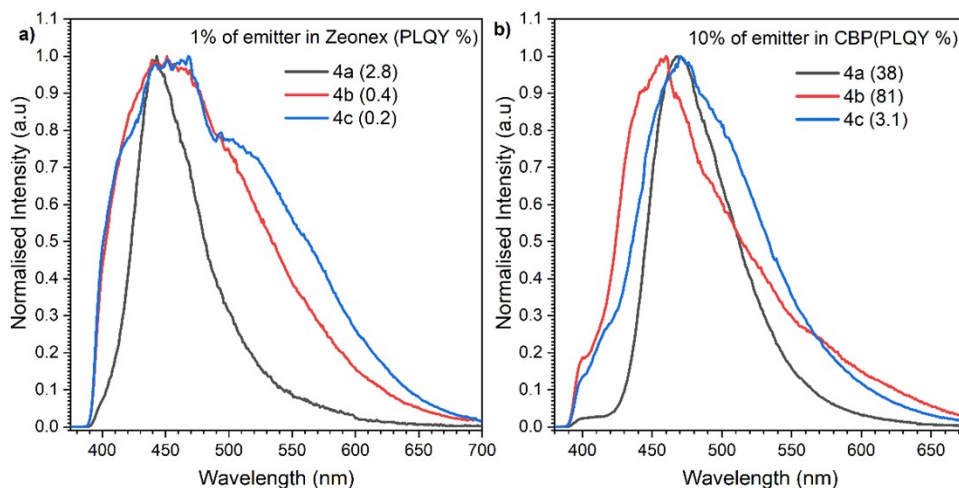


Figure S11. Steady-state PL emission of **4a-4c** in ambient condition: 1 wt% of emitter in Zeonex (a); 10 wt% of emitters in CBP; PLQY was measured at ambient condition. Spectra were recorded at 300K using $\lambda_{\text{ex}} = 355 \text{ nm}$.

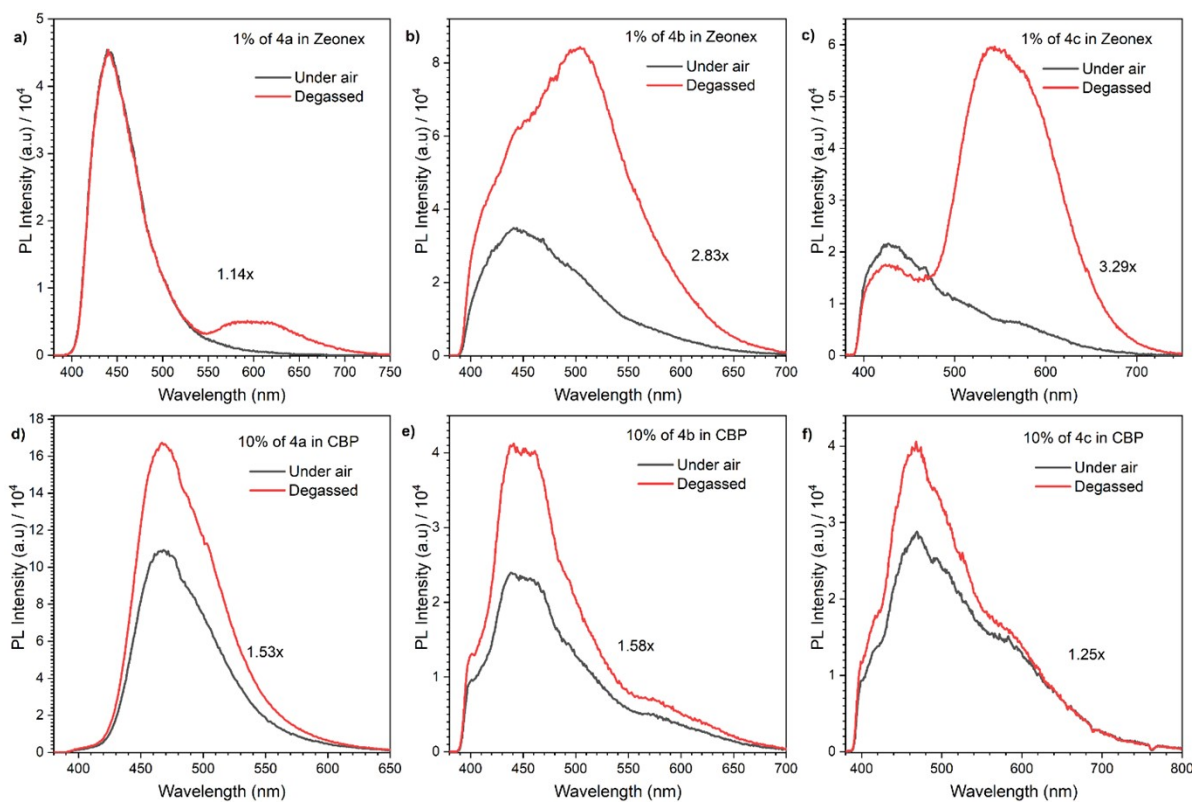


Figure S12. Steady-state photoluminescence (PL) spectra in Zeonex® in the presence of air (Under air) and in a vacuum (degassed) for the compounds **4a-4c**. Recorded at 300 K using $\lambda_{\text{ex}}=355 \text{ nm}$.

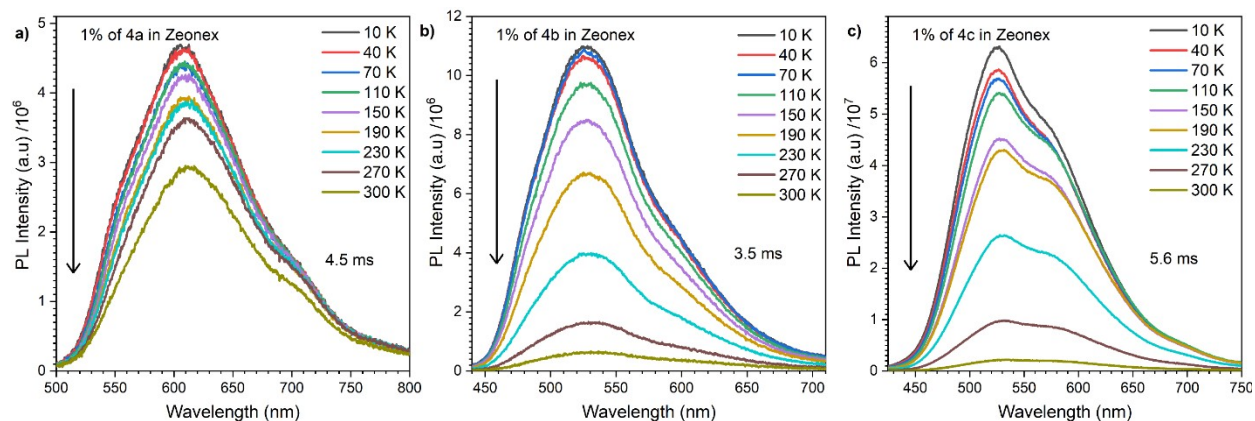


Figure S13. Temperature dependent time resolved PH spectra of the 1wt% of emitters (**4a-4c**) in Zeonex and $\lambda_{ex}=355$ nm.

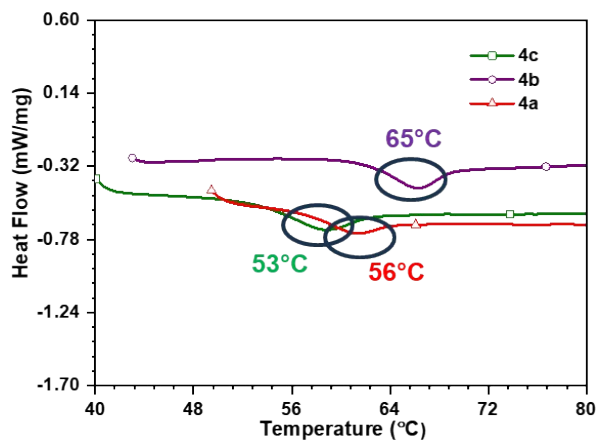
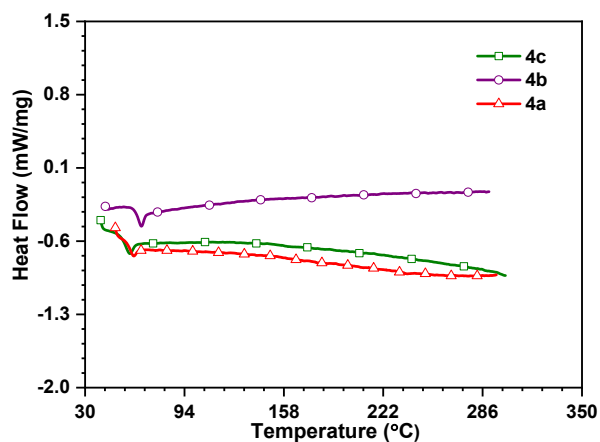


Figure S14. Differential scanning calorimetry

(DSC) traces of **4a**, **4b** and **4c**.

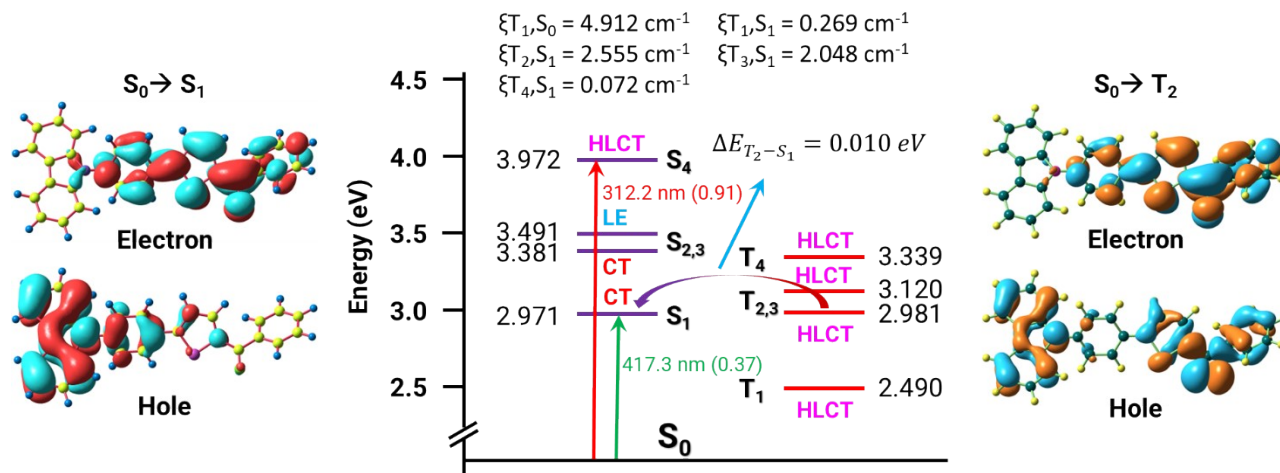


Figure S15. Energy level diagram of 4a.

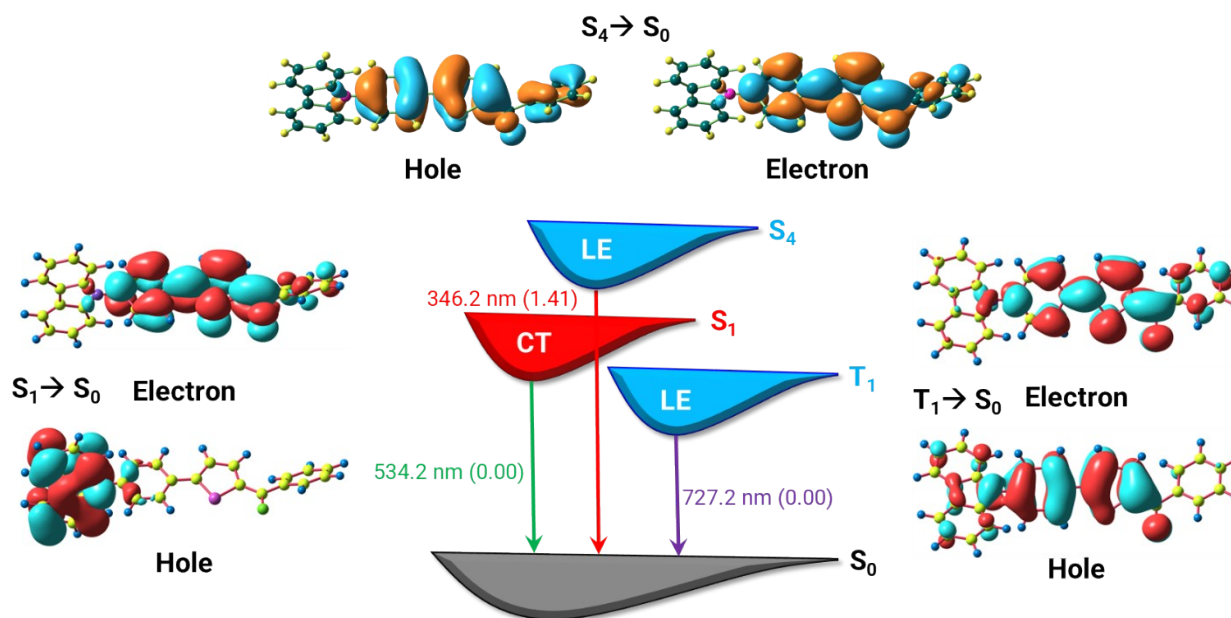


Figure S16. Emission NTO analysis of 4a.

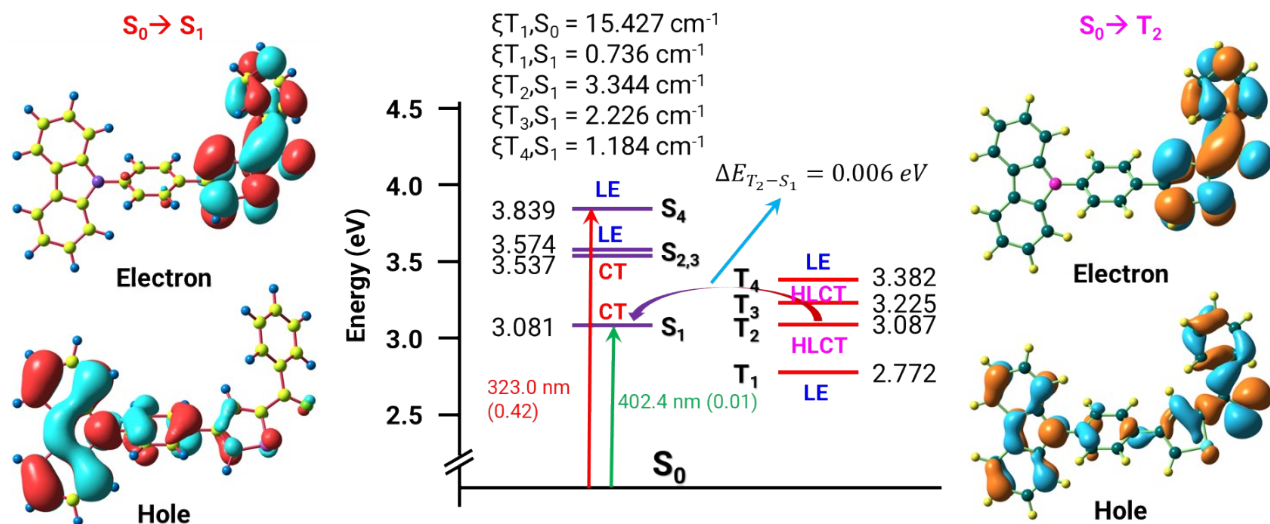


Figure S17. Energy level diagram of 4b.

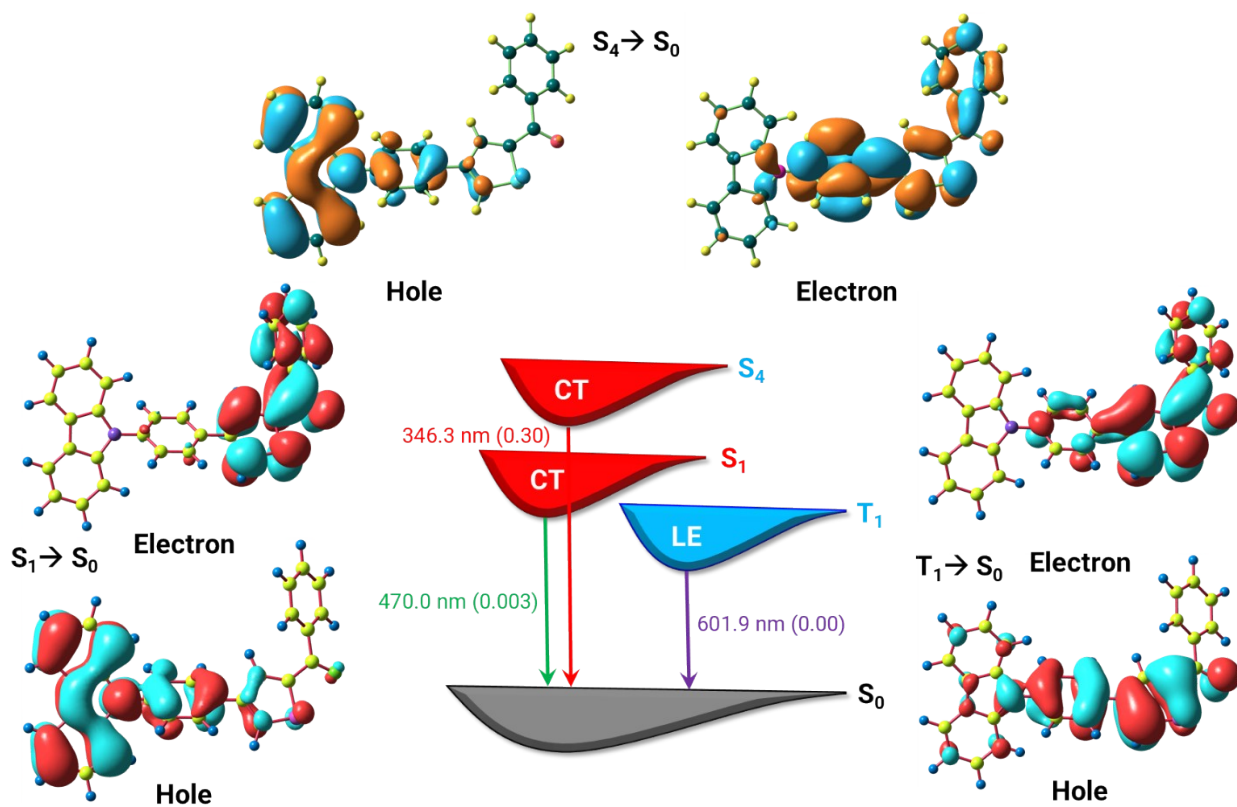


Figure S18. Emission NTO analysis of 4b.

Single Crystal Analysis

Table S6. Crystal data and structure refinement data for 4a	
Identification code	4a
CCDC	2516523
Empirical formula	C ₂₉ H ₁₉ NOS
Formula weight	429.51
Temperature/K	100.00
Crystal system	monoclinic
Space group	P2 ₁ /c
a/Å	25.2496(12)
b/Å	13.1469(6)
c/Å	25.8557(13)
α/°	90
β/°	95.084(2)
γ/°	90
Volume/Å³	8549.1(7)
Z	16
ρ_{calc}/cm³	1.335
μ/mm⁻¹	0.174
F(000)	3584.0
Crystal size/mm³	0.41 × 0.24 × 0.069
Radiation	MoKα (λ = 0.71073)
2θ range for data collection/°	3.162 to 54.976
Index ranges	-32 ≤ h ≤ 32, -17 ≤ k ≤ 17, -33 ≤ l ≤ 33
Reflections collected	224007
Independent reflections	19513 [R _{int} = 0.0870, R _{sigma} = 0.0455]
Data/restraints/parameters	19513/0/1153
Goodness-of-fit on F²	1.040
Final R indexes [I ≥ 2σ (I)]	R ₁ = 0.0428, wR ₂ = 0.0953
Final R indexes [all data]	R ₁ = 0.0633, wR ₂ = 0.1095
Largest diff. peak/hole / e Å⁻³	0.29/-0.30

Table S7. Crystal data and structure refinement data for 4b	
Identification code	4b
CCDC	2516522
Empirical formula	C ₂₉ H ₁₉ NOS
Formula weight	429.51
Temperature/K	273.15
Crystal system	monoclinic
Space group	P2 ₁ /n
a/Å	15.597(5)
b/Å	7.801(2)
c/Å	17.993(6)
α/°	90
β/°	96.173(10)
γ/°	90
Volume/Å³	2176.7(11)
Z	4
ρ_{calc}/g/cm³	1.311
μ/mm⁻¹	0.171
F(000)	896.0
Crystal size/mm³	0.256 × 0.136 × 0.086
Radiation	MoKα (λ = 0.71073)
2θ range for data collection/°	5.698 to 56.63
Index ranges	-20 ≤ h ≤ 20, -10 ≤ k ≤ 10, -23 ≤ l ≤ 23
Reflections collected	32640
Independent reflections	5390 [R _{int} = 0.0939, R _{sigma} = 0.0589]
Data/restraints/parameters	5390/0/289
Goodness-of-fit on F²	1.044
Final R indexes [I ≥ 2σ(I)]	R ₁ = 0.0474, wR ₂ = 0.1107
Final R indexes [all data]	R ₁ = 0.0679, wR ₂ = 0.1253
Largest diff. peak/hole / e Å⁻³	0.28/-0.33

Table S8. Crystal data and structure refinement data for 4c	
Identification code	4c
CCDC	2516524
Empirical formula	C ₃₀ H ₂₃ NO ₂ S
Formula weight	461.55
Temperature/K	296.15
Crystal system	monoclinic
Space group	C2/c
a/Å	41.689(5)
b/Å	7.5671(9)
c/Å	34.585(4)
α/°	90
β/°	121.555(3)
γ/°	90
Volume/Å³	9297.1(19)
Z	16
ρ_{calc}/g/cm³	1.319
μ/mm⁻¹	0.168
F(000)	3872.0
Crystal size/mm³	0.216 × 0.119 × 0.109
Radiation	MoKα (λ = 0.71073)
2θ range for data collection/°	3.924 to 53.382
Index ranges	-52 ≤ h ≤ 52, -9 ≤ k ≤ 9, -43 ≤ l ≤ 39
Reflections collected	57410
Independent reflections	9762 [R _{int} = 0.1049, R _{sigma} = 0.0798]
Data/restraints/parameters	9762/0/578
Goodness-of-fit on F²	1.197
Final R indexes [I ≥ 2σ (I)]	R ₁ = 0.1174, wR ₂ = 0.2105
Final R indexes [all data]	R ₁ = 0.1430, wR ₂ = 0.2218
Largest diff. peak/hole / e Å⁻³	0.55/-0.40

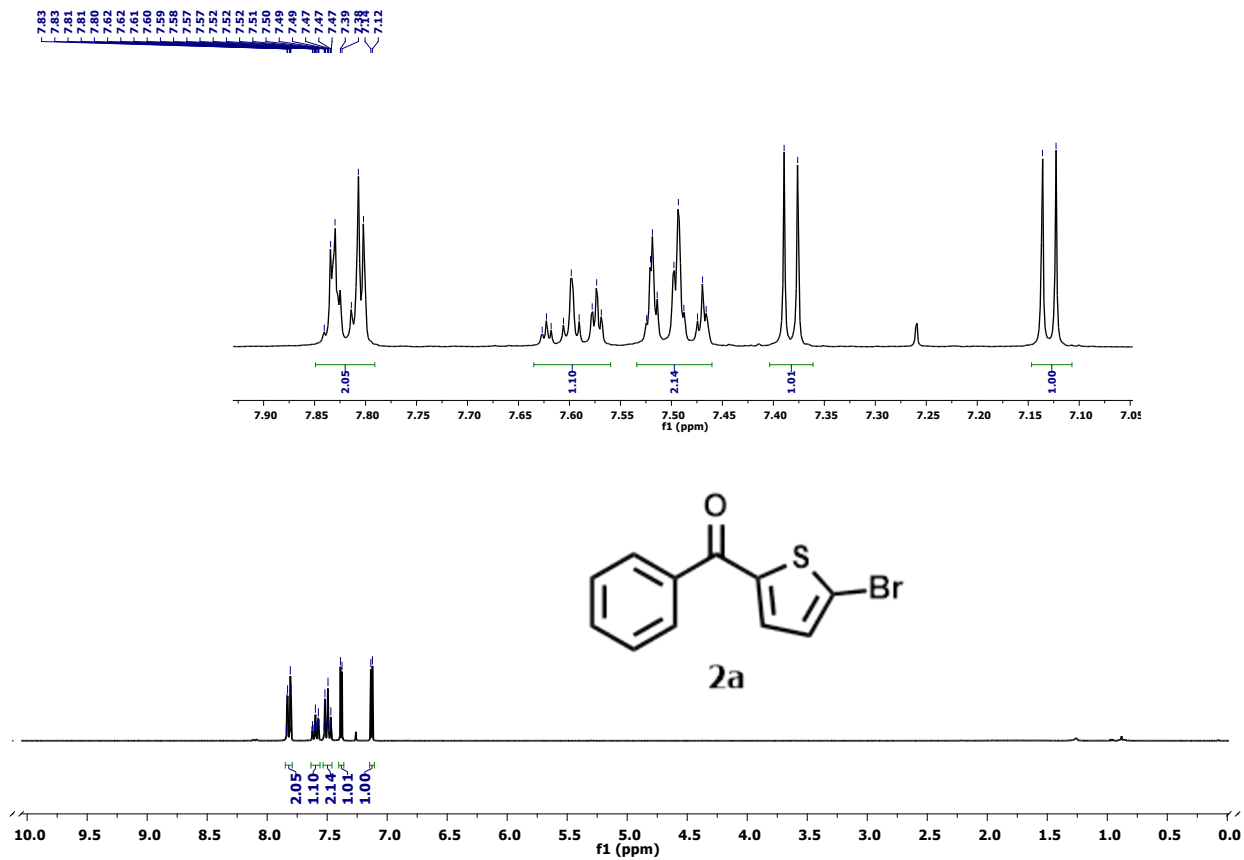


Figure S19. ^1H NMR spectrum of **2a** recorded in CDCl_3 .

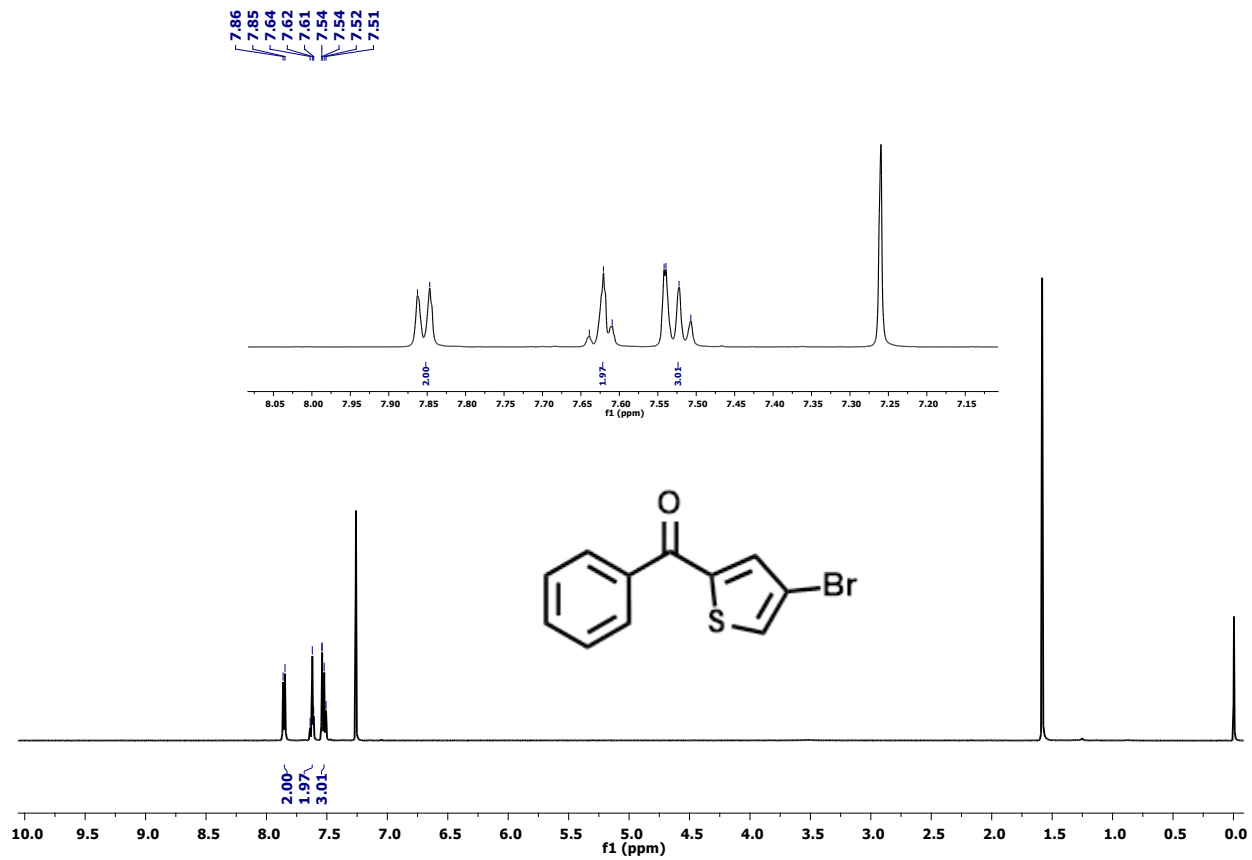


Figure S20. ^1H NMR spectrum of **2b** recorded in CDCl_3 .

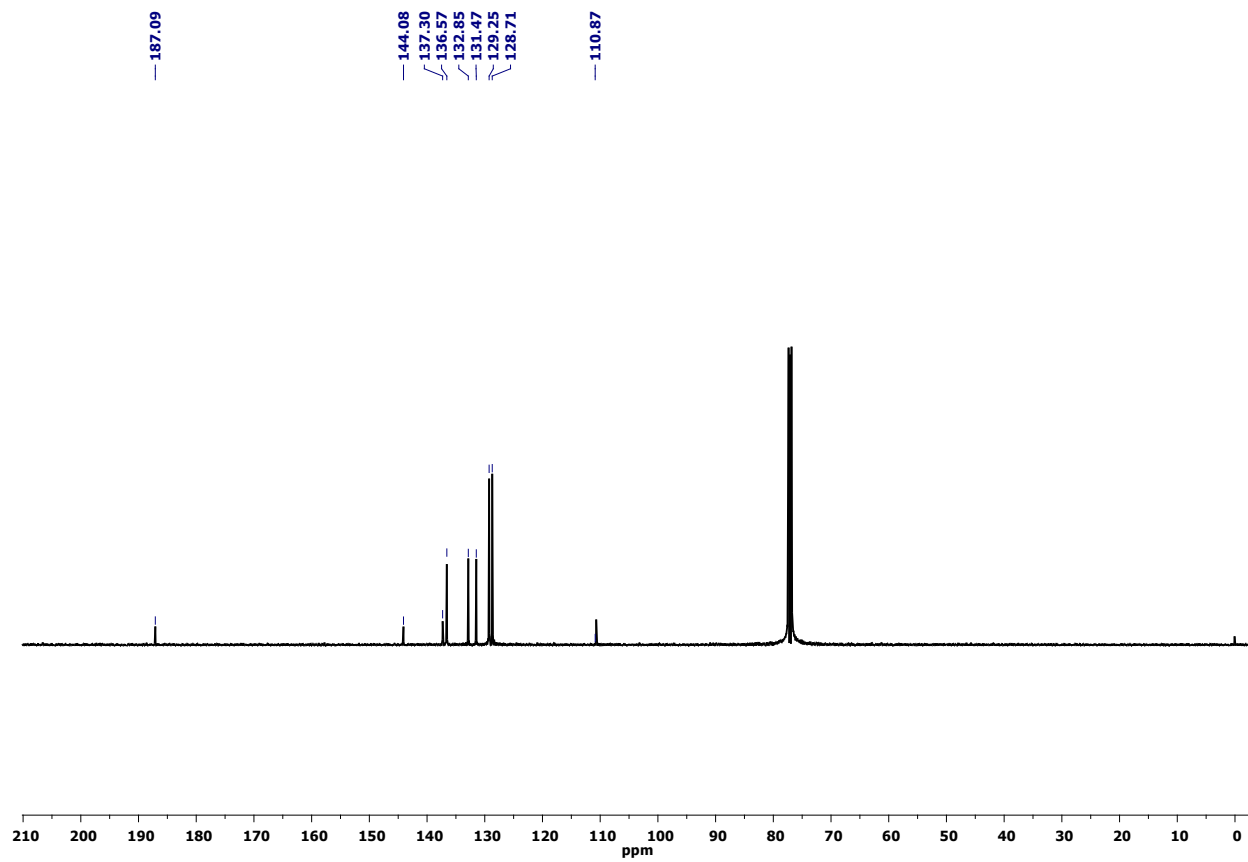


Figure S21. ^{13}C NMR spectrum of **2b** recorded in CDCl_3 .

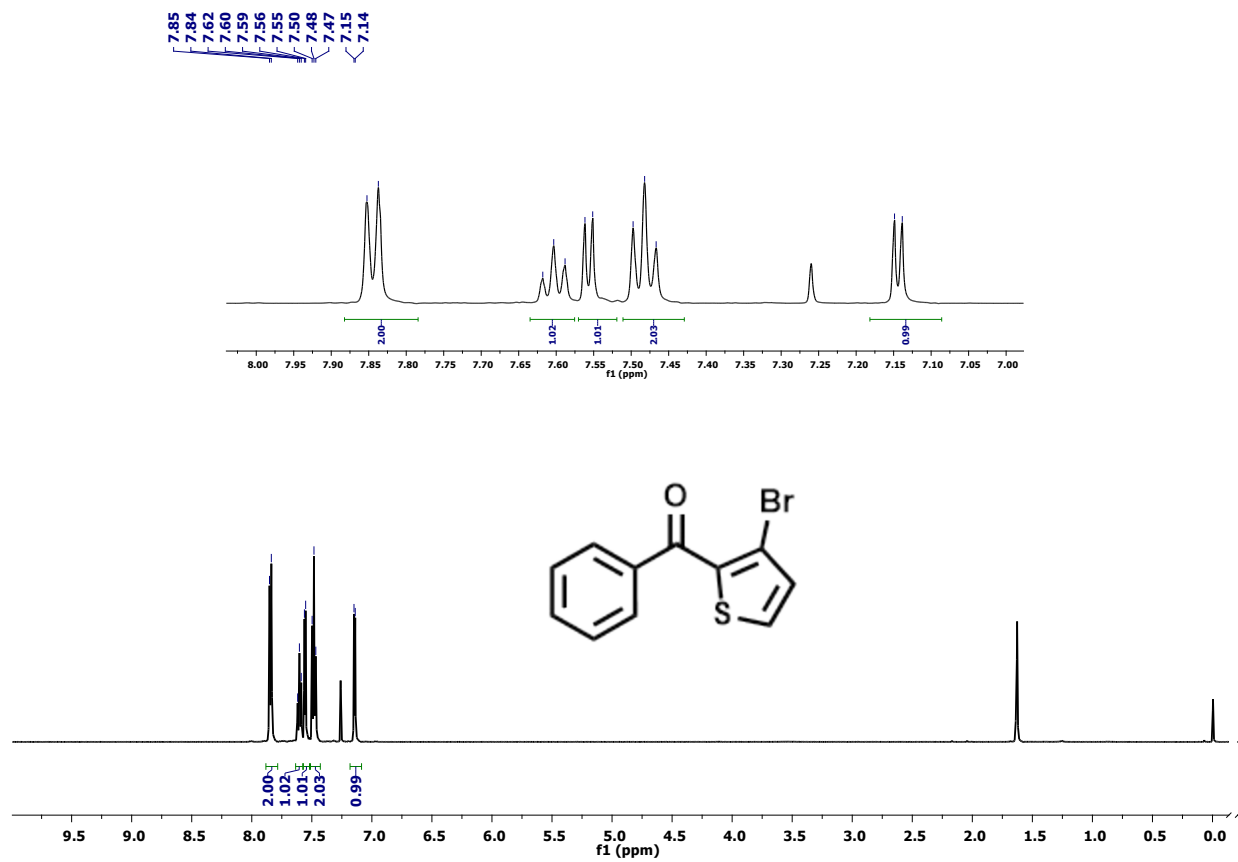


Figure S22. ¹H NMR spectrum of **2c** recorded in CDCl₃.

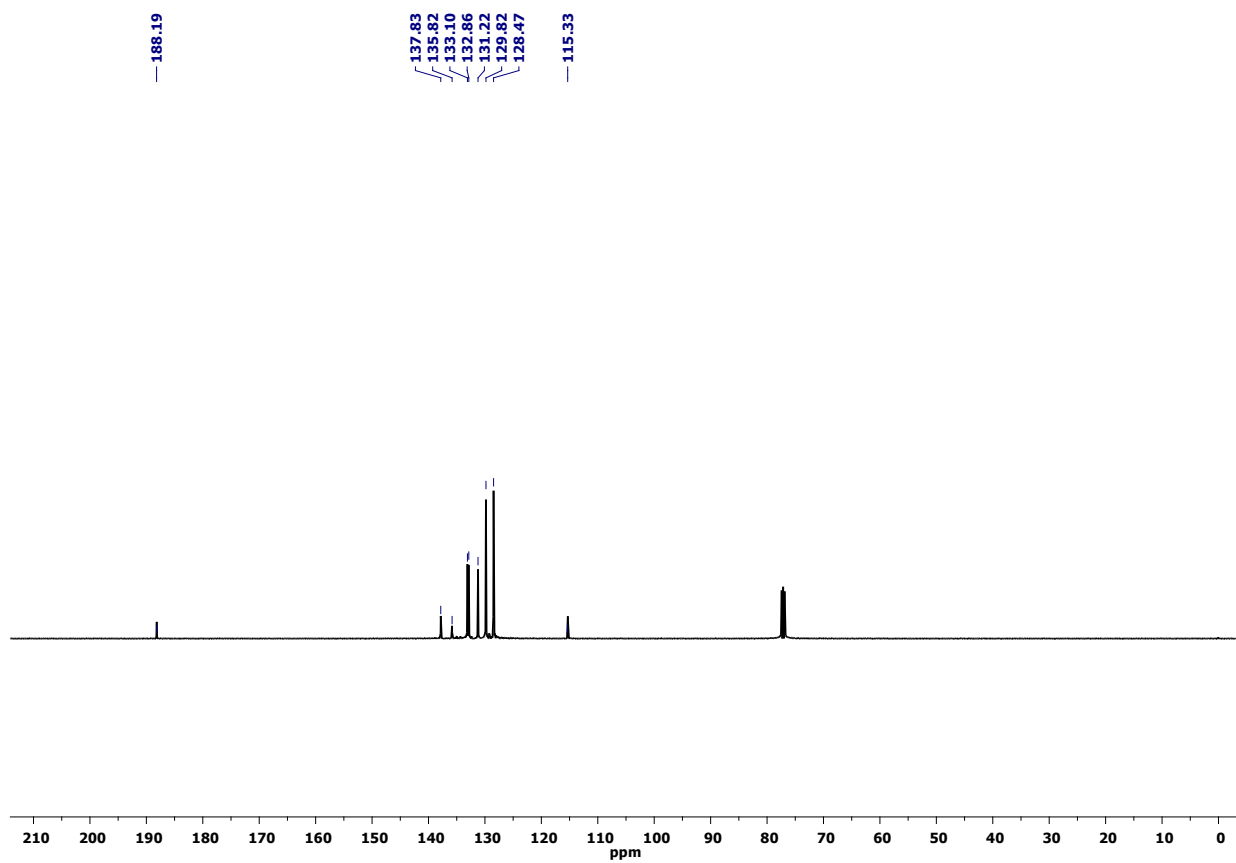


Figure S23. ^{13}C NMR spectrum of **2c** recorded in CDCl_3 .

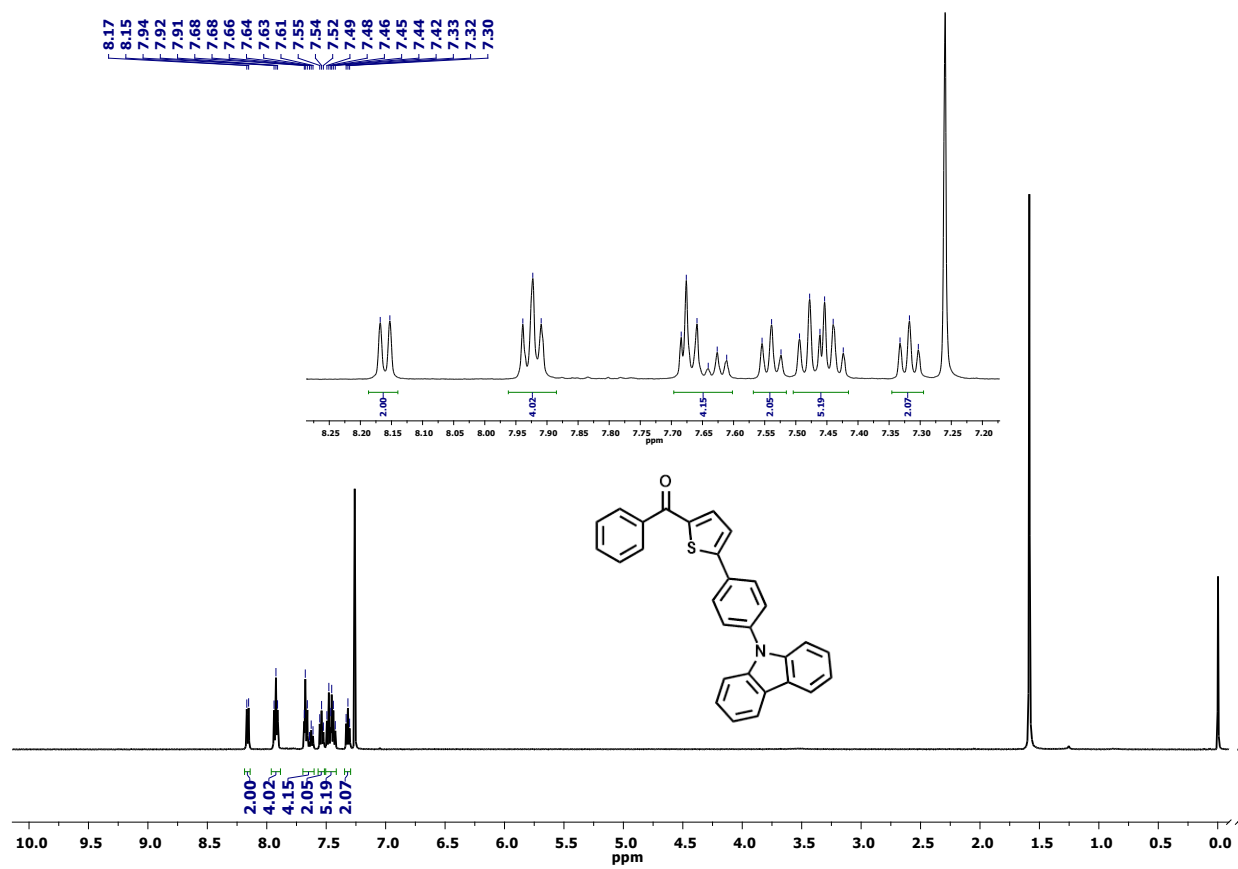


Figure S24. ¹H NMR spectrum of **4a** recorded in CDCl₃.

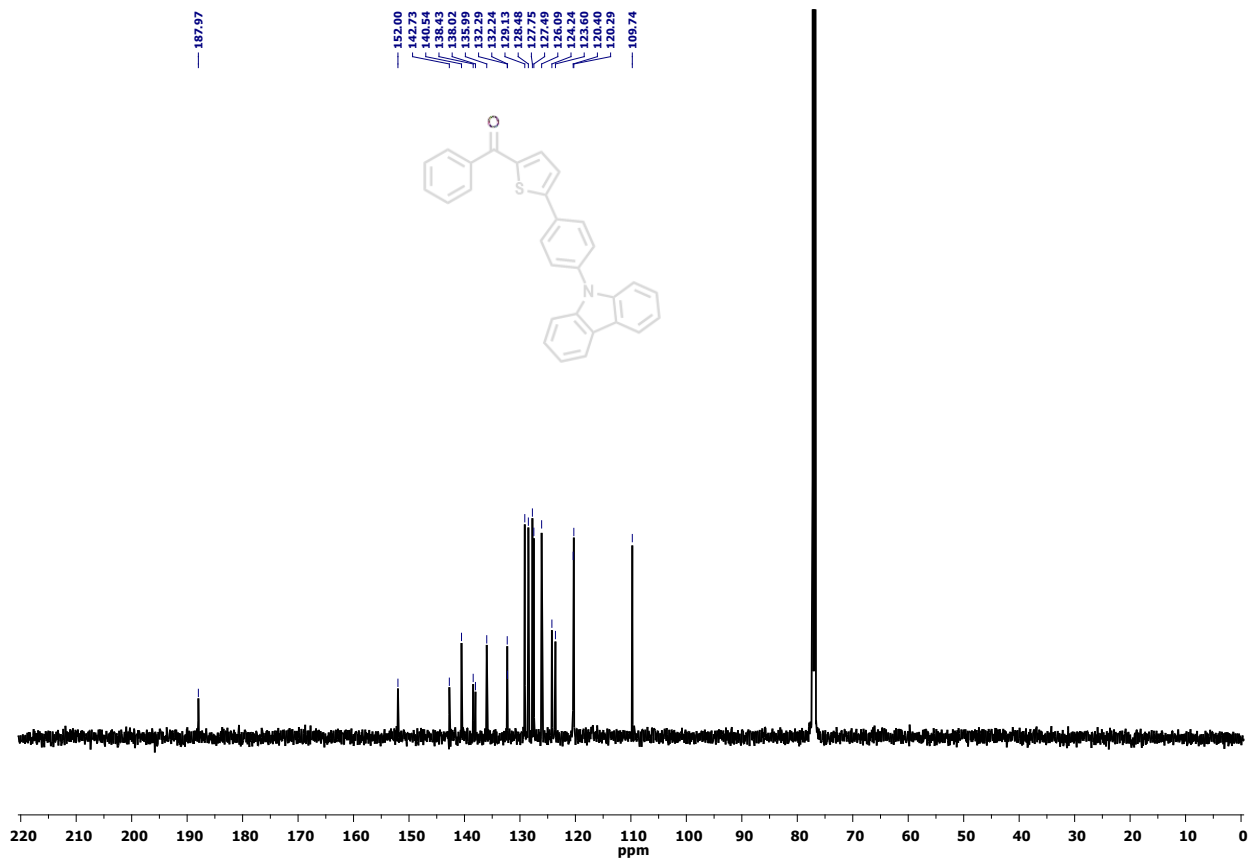


Figure S25. ¹³C NMR spectrum of **4a** recorded in CDCl₃.

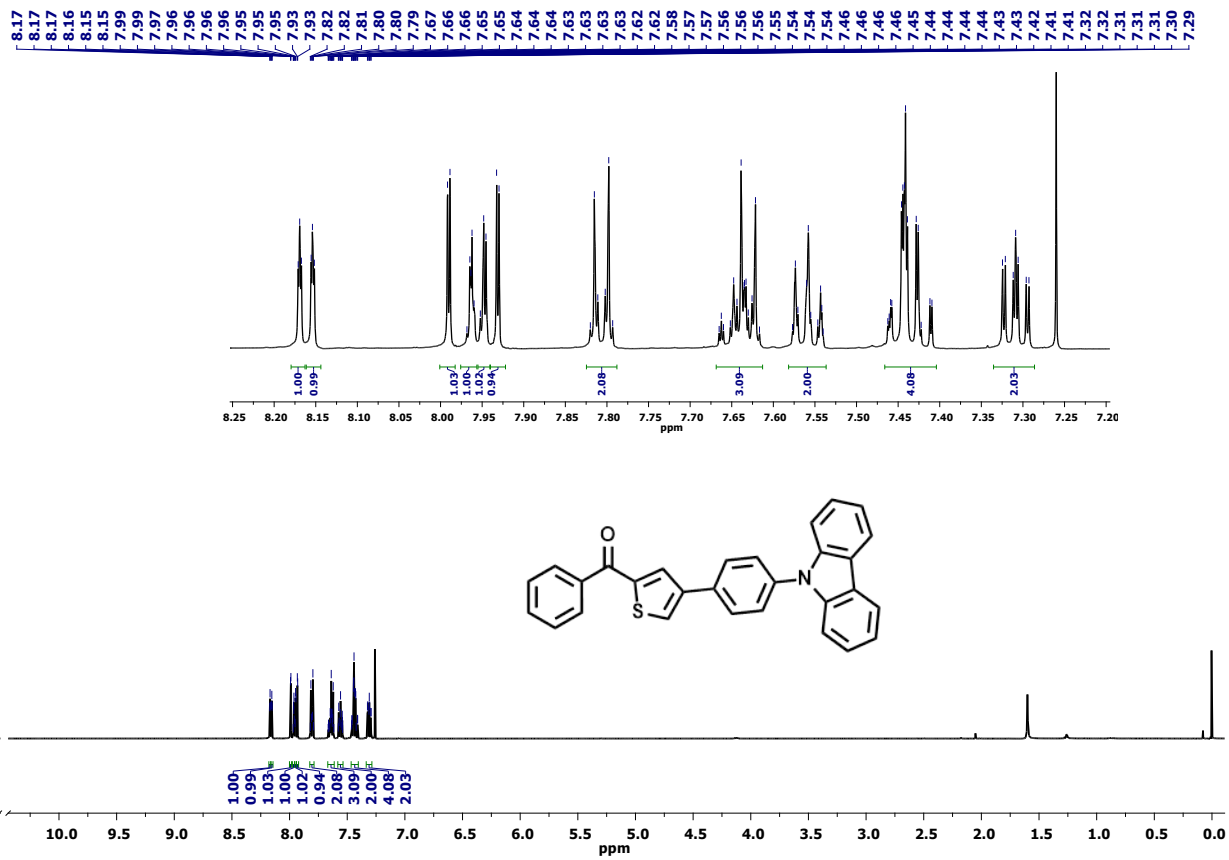


Figure S26. ¹H NMR spectrum of **4b** recorded in CDCl₃.

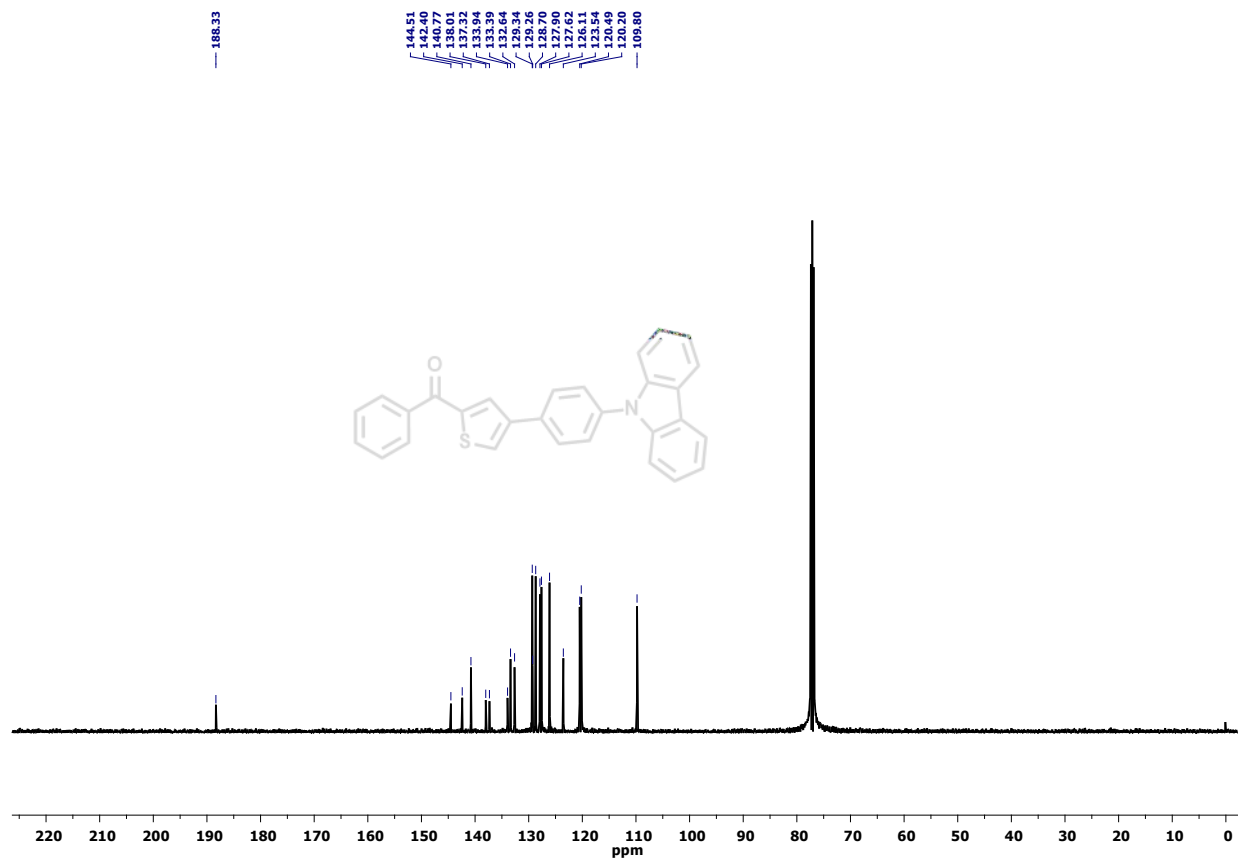


Figure S27. ^{13}C NMR spectrum of **4b** recorded in CDCl_3 .

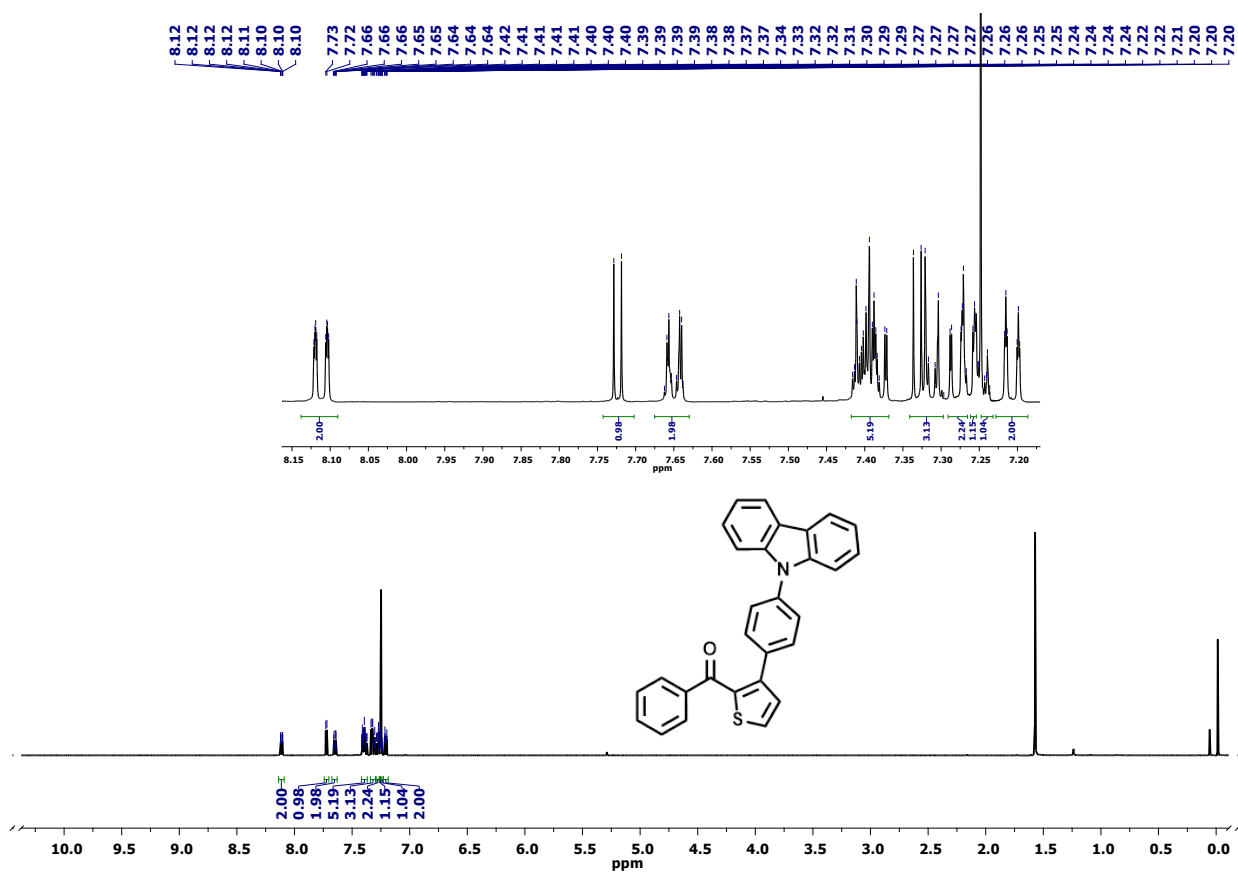


Figure S28. ¹H NMR spectrum of **4c** recorded in CDCl₃.

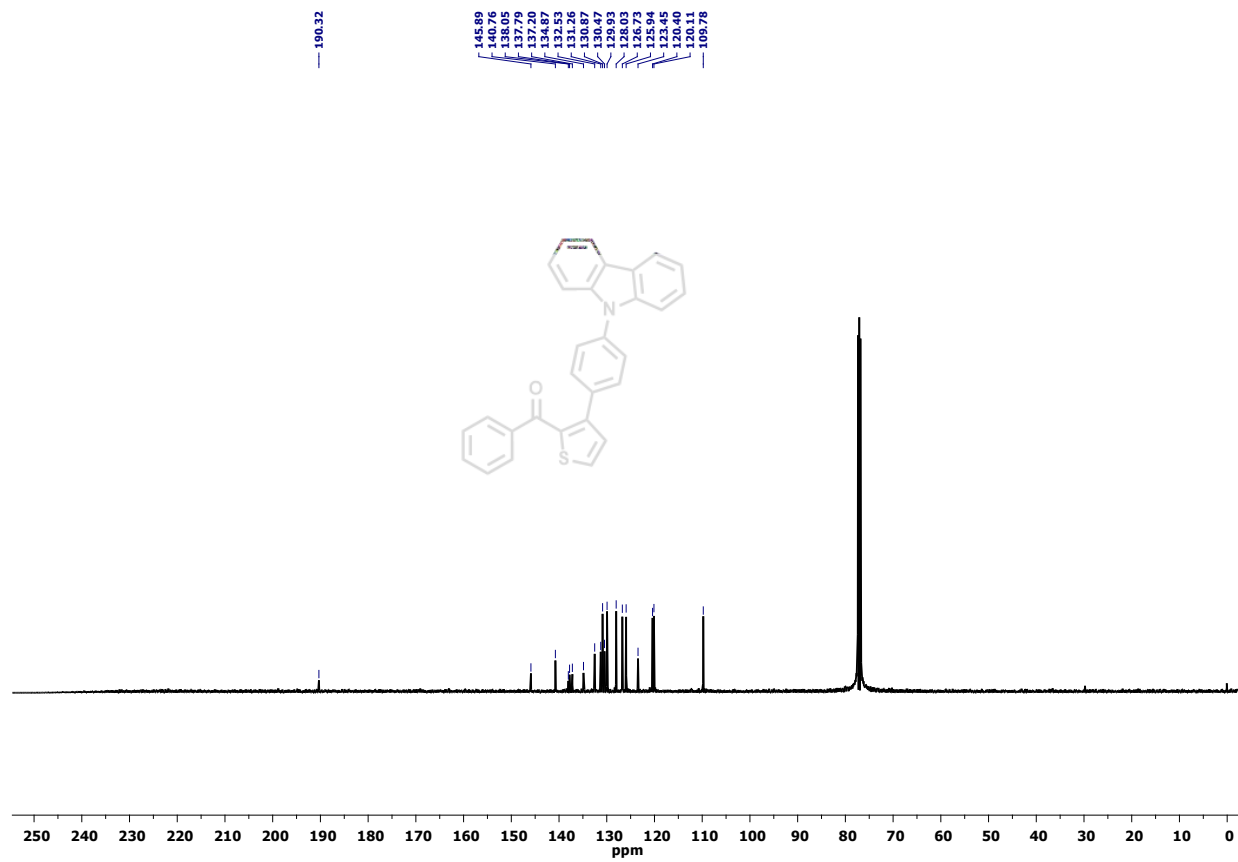


Figure S29. ^{13}C NMR spectrum of **4c** recorded in CDCl_3 .

REFERENCES

1. J. A. Letizia, A. Facchetti, C. L. Stern, M. A. Ratner, T. J. Marks, High electron mobility in solution-cast and vapor-deposited phenacyl-quaterthiophene-based field-effect transistors: toward *n*-type polythiophenes, *J. Am. Chem. Soc.*, 2005, **127**, 13476.
2. F. Neese, Software update: the ORCA program system -- Version 5.0, *WIREs Comput. Molec. Sci.*, 2022, **12**, e1606. (DOI: 10.1002/wcms.1606)